Remembering what is relevant: how is goal-directed memory reactivation supported by attention and working memory?

Melinda Sabo[1*], Edmund Wascher[1], Daniel Schneider[1]

[1] Leibniz Research Centre for Working Environment and Human Factors,
Ardeystraße 67, 44139 Dortmund, Germany

Author Note

Melinda Sabo https://orcid.org/0000-0001-8585-7115

Edmund Wascher https://orcid.org/0000-0003-3616-9767

Daniel Schneider https://orcid.org/0000-0002-2867-2613

Correspondence concerning this article should be addressed to Melinda Sabo,

Leibniz Research Centre for Working Environment and Human Factors, Ardeystraße 67

44139 Dortmund, Germany

E-mail: sabo@ifado.de

Abstract

Goal-directed memory reactivation involves the prioritization of information relevant for the current behavioral goal and it was argued to elicit fronto-parietal network activity. Yet, the exact processes underlying goal-directed memory reactivation remain unclear. We suggest that attention might be a potential candidate fulfilling this role, thus we aimed to examine how attentional mechanisms are involved in goal-directed memory reactivation, by studying cortical activity at the scalp level via electroencephalogram (EEG). We designed an eLTM experiment, in which subjects were required to learn associations between objects and two locations on the screen. In order to capture adaptations to a new set of goals (thus manipulating the goal-directed nature of memory), the relevance of some of the originally encoded locations changed in the second phase of the experiment. As such, subjects were presented two types of cues: the neutral cue suggested that both positions are still relevant, while the selective cue indicated that only *one* previous location remained relevant. Regarding the EEG correlates, modulations of lateralized alpha-beta and non-lateralized delta-to-theta power, as well as lateralized anterior and posterior event-related components were examined. In addition, multivariate pattern analyses were also adopted. Our results suggest that after initial reactivation from eLTM, attentional mechanisms support the selection of the task-relevant information in line with the behavioral goals. Moreover, we argue that the reactivated location information is temporarily stored in working memory, where attentional processes act upon it. We conclude that these results have important implications with respect to the information exchange between the short-term and long-term memory systems.

Keywords: *episodic long-term memory, incidental reactivation, neural oscillations, relevance manipulation, goal-directed behavior*

1. Introduction

An impressive feature of our episodic long-term memory (eLTM) relies in its capacity to encode numerous details associated with a particular event. These details are later automatically reactivated as part of the original episode, although some of them may be irrelevant for the current behavior. This phenomenon of reactivating all original features of an episode has been termed as incidental memory reactivation and it was argued to differ from goal-directed memory reactivation, which entails only the retrieval of information important for the current behavioral goals (Kuhl et al., 2013). These two concepts were not only differentiated at a theoretical level, but dissociated at a neural level, as well. As such, previous research found that the fronto-parietal network represents reactivated information more selectively in accordance with behavioral goals (Kuhl et al., 2013; Long & Kuhl, 2018), while the ventral medial temporal cortex proved to be less selective and supported both relevant and irrelevant information retrieval (i.e., incidental reactivation) (Kuhl et al., 2013). This finding is in line with the account suggested by Sestieri and colleagues (2017), who argue that automatic (i.e., incidental reactivation in Kuhl and colleagues' terminology) and goal-directed reactivation are two different sub-processes of eLTM retrieval. As such, in their view, the medial temporal lobe (MTL) supports the early information reactivation phase, which is followed by information maintenance for which the angular gyrus (AG) is responsible. Subsequently, the LTM content is subjected to transformations and manipulations in line with current task demands, which is coordinated by the lateral inferior parietal sulcus and (latIPS) and post-central sulcus (PoCS), both part of the fronto-parietal control network (Sestieri et al., 2017). Although these studies establish the involvement of different posterior parietal cortex (PPC) sub-regions at different stages of eLTM retrieval, it is not clear what kind of processes support these transformations of eLTM content after initial reactivation.

Based on previous research, it is reasonable to assume that selective attention is an important candidate fulfilling this role. Accordingly, it has been argued that tasks requiring only one piece of information from multiple retrieved LTM associations elicit inferior parietal lobule activations (Kizilirmak et al., 2015). This activity pattern was interpreted as attentional reorienting supporting the selection of task-relevant information. In a different study incentivizing the retrieval of only certain encoded information (thus manipulating top-down goals), target memory retrieval was again associated with parietal lobe activity, more specifically in the superior parietal lobule, a region involved in the top-down attentional network (Ciaramelli et al., 2020). Furthermore, in a design which manipulated the relevance of retrieved associations, Jost and colleagues (2012) found that both task-relevant and irrelevant associations were automatically retrieved, thus creating interference. The authors argue that target enhancement was an additional mechanism through which conflict was reduced. Although the exact process was not discussed in detail, it can be assumed that attentional selection mediated conflict resolution, since it was previously argued that target enhancement is a sub-process of attentional selection (cf., Schneider et al., 2022).

Collectively, this line of research points towards the important role of attentional selection during eLTM retrieval. In the present work, we seek to experimentally test this assumption and to provide a better understanding of the processes facilitating goal-directed memory reactivation by recording cortical activity changes via EEG. While the current study is not the only one adopting EEG for examining eLTM retrieval process, an important feature differentiating it from previous ones, is the relevance manipulation introduced to our eLTM task. This manipulation allows us to investigate top-down attentional mechanisms, unfolding as a result of initially encoded information losing its relevance. Regarding similar EEG studies conducted before, Waldhauser and colleagues (2012) indicated that inhibition of irrelevant long-term memory content mediates interference resolution during eLTM retrieval,

a conclusion supported by topographic modulations of alpha-beta power (~8-30 Hz). This previous investigation captured an early and automatic inhibitory process, which occurred in the context of retrieval induced forgetting. Yet here, we examine how already encoded eLTM content is prioritized in line with new task requirements introduced after initial encoding. We argue that this prioritization process should be based on deliberate, top-down driven attentional focusing, as opposed to an automatic process occurring during retrieval. As such, in our design, we require participants to first associate two spatial locations with an object. To be able to inspect the processes involved in goal-directed memory retrieval, we changed some of the locations' relevance in the phase subsequent to encoding (i.e., cuing phase). Here, for certain objects, a cue indicated that only one of the two locations will be relevant (selective cue), while the rest of the objects were still supposed to be associated with the two initial locations (i.e., neutral cue) (see Figure 1).

We hypothesize that attentional processes acting upon the retrieved eLTM information underlie the relevance changes of the originally encoded eLTM associations. This entails that all locations linked to an object (here: acting as retrieval cue) are reactivated from eLTM before attentional control mechanisms would bias further processing towards the task-relevant content. Moreover, we expect that the EEG patterns will be comparable to those observed in previous investigations studying attentional selection of information reactivated from working memory (WM; e.g., Poch et al., 2018).

One important EEG correlate previously linked to such attentional modulations is alpha power activity calculated relative to the location of the target and non-target item. For example, de Vries and colleagues (2018) showed that when two initially encoded WM representations are relevant at different time points within a trial, attentional selection elicits a stronger contralateral (as compared to ipsilateral) alpha (8-14 Hz) suppression relative to the currently relevant item, indicating that this information is prioritized (i.e., target facilitation).

Similarly, when the WM representation was no-more or not-yet-relevant, an increase in alpha power contralateral (as compared to ipsilateral) to the item's location was observed (i.e., non-target or distractor inhibition; see also Rösner et al., 2020; Schneider et al., 2019). In light of these previous findings, we designed our experiment in a way that allows an independent examination of the alpha power asymmetry relative to the cued vs. non-cued location. As such, only one of the these two positions was lateral (i.e., left or right), while the other one was non-lateral (top vs. bottom without lateral offset). In this context, following the presentation of the selective cues, we expected an alpha-beta (~8-20 Hz) power suppression contralateral to the cued location and an increase in alpha-beta power contralateral to the non-cued location, indicating selective attentional orienting.

In addition to the above-mentioned oscillatory effects, attentional selection should be also reflected in lateralized event-related potentials (ERP) previously observed in comparable scenarios at the level of WM. As such, ERP modulations were found over both posterior and anterior cortical areas when visual information stored in WM was selected for further processing. This posterior effect is analogous to the N2 posterior contralateral component (N2pc; see Luck & Hillyard, 1994) initially studied in the context of visual search. It is characterized by a stronger negativity at posterior lateral electrodes relative to the cued information (e.g., Salahub et al., 2019). In addition to the N2pc component, previous studies also observed negative-going activity occurring at frontal lateral electrodes, stronger contralateral (as compared to ipsilateral) to the location, on which selected information was presented during encoding (e.g., Myers et al., 2015; Schneider et al., 2016). This effect was previously referred to as anterior directing attention negativity (ADAN, Eimer et al., 2002).

Finally, since our design aims to explore how the memory system handles and adapts to changes in the relevance of already encoded LTM information, modulations of oscillatory power in the theta frequency range will be also considered. Originally, mid-frontal theta

power changes were observed in scenarios requiring conflict monitoring and interference resolution (Cavanagh & Frank, 2014). However, more recent studies argue that mid-frontal theta activity rather reflects a general need for cognitive control, observed for instance in tasks requiring goal updating (Cooper et al., 2017). In addition, it was also suggested that delta-to-theta power modulations reflect a higher-level control process for orchestrating the attentional prioritization of WM content (de Vries et al., 2018). Regarding the current study, we expect that such a higher-level control mechanism will also be involved in coordinating attentional selection during eLTM retrieval. Therefore, we expect a stronger oscillatory power in the delta-theta frequency range (~2-5 Hz) in the selective cue condition (as compared with the neutral cue condition), indicating the increased need for attentional control when selecting one, out of two object-location associations for a later retrieval task.

2. Methods

2.1. Participants

Initially 32 participants took part in the study. Since the instructions were provided in German and not all participants were native German speakers, two participants misunderstood the instructions, thus did not properly do the encoding of the object-location associations. These two datasets were excluded from further analyses so that 30 participants (age range: 18-29 years, *M* = 23.5 years, SD = 2.84 years) were included in the final sample (16 females, 14 males). All subjects were right-handed (as assessed by the Edinburgh Handedness Inventory; Oldfield, 1971), had normal or corrected-to-normal vision and declared not suffering from any psychiatric or neurological disorder. Written consent was obtained from all subjects before the start of the experiment. Participation was compensated with 10 Euros/hour or study completion credits (in case of psychology students). The study was conducted in accordance with the Declaration of Helsinki and was authorized by the

ethics committee of the Leibniz Research Centre for Working Environment and Human Factors (Dortmund, Germany).

2.2. Procedure

Upon arrival, subjects were provided with general information about the study. Subsequently, they filled in a demographic questionnaire, together with the Edinburgh Handedness Inventory (Oldfield, 1971). Afterwards, the EEG cap was prepared, and participants were seated in the dimly lit, sound attenuated, and electrically shielded EEG chamber. The experiment was done on a 22-inch CRT monitor (100 Hz; 1024 × 768 pixels) and the viewing distance from the monitor was ~145 cm. The task consisted of a training, followed by the three-phase eLTM experiment. Between phases, subjects had three-minutes breaks, with a three-minute distractor task in-between. Once the task was finalized, participants were administered a follow-up questionnaire, in which they were asked about the used strategy and the encountered difficulties. Half of the subjects also completed an intelligence test subsequently; however this is outside the scope of the current study. The duration of the whole procedure was ~3-3.5 h.

2.3. Experimental procedure

2.3.1. Stimulus materials

For each participant, 120 objects were randomly chosen from a stimulus pool consisting of everyday objects (Rossion & Pourtois, 2004). The original stimulus pool contained 260 objects, but based on the image rating survey we conducted in a previous study (Sabo & Schneider, 2022) we only considered a sub-sample of 240 objects, which had the best luminance, contrast, vividness, and were the most easily recognizable.

2.3.2. Episodic-long-term memory task

The main task of the current experiment involved three major phases: an encoding-, a cuing-, and a retrieval phase. These phases were separated by a three-minute distractor task (counting backwards in steps of three starting from 500) and two breaks, each consisting of three minutes, leading to a total of nine minutes. The experiment was introduced by a short training, which aimed to familiarize participants with the task. The training included seven objects and it was identical to the main experiment in terms of instructions.

In the encoding phase, subjects were presented with an object (size: 4.3° × 2.9° or 2.9° × 4.3°) appearing on a gray background (RGB 128-128-128). The object was shown for 500 ms and could occur on four possible locations on the screen: top, bottom, left or right. Subjects' task was to memorize the association between the object and its presentation location, while fixating on the centrally presented black dot (size: 0.2° × 0.2°, distance between the object and the central fixation dot: 3°) (see Figure 1). Participants were instructed to use a specific strategy for memorizing the object-presentation location association. More specifically, after the object disappeared from the screen, they were supposed to visualize the object on the corresponding presentation location, while still maintaining their gaze on the central fixation dot. Furthermore, they were instructed not to repeat the associations verbally or to rely on semantic information. The memorization of an association was confirmed by clicking the mouse button with the index finger of the right hand, which led to the start of the next trial. If a participant assigned more than 15 s throughout multiple consecutive trials for the memorization of an association, they were verbally instructed to proceed faster. During the encoding phase, each of the 120 objects was associated with two presentation locations: a lateral location (left or right) and a non-lateral one (top or bottom). In order to facilitate the learning process, each object-presentation

location association occurred twice during encoding, leading to a total of 480 trials (organized in eight blocks). Between these blocks, self-paced breaks were introduced.

The cuing phase started with the central presentation of a previously seen object. After 500 ms, a set of four circles (size: 2°), serving as a cue, appeared on the screen (distance between the object and the circles in visual angle: 3°). The reason why we introduced a 500 ms time window between the object and the cue onset was due to the separation of reactivation processes from other (attentional) mechanisms triggered by the cue presentation. Regarding the cues, they could be presented in one of the following configurations: (i) two blue circles (RGB: 50-85-150) along the vertical axis (i.e., top and bottom locations; selective cue); (ii) two blue circles (RGB: 50-85-150) along the horizontal axis (i.e., left and right locations; selective cue); (iii) four gray circles (RGB: 200-200-200) on top, bottom, left, and right locations (neutral cue; see also Figure 1). In the first case, subjects' task was to retrieve and selectively associate the object with the location situated along the vertical axis (selective cue condition). For instance, if an object was linked to the locations top and left during encoding (see Figure 1), in the cuing phase, subjects were required to associate only the top location with the respective object. In the second selective condition, only the location situated along the horizontal axis (i.e., left or right) was relevant. Finally, in the neutral condition, both locations originally linked to the object remained relevant. One third of the objects (40 in total) were assigned to the horizontal selective cue condition, another one third (40 in total) to the vertical selective cue condition, while the remaining 40 objects to the neutral cue condition. Similar to the encoding phase, the memorization of an association was confirmed by a mouse button click with the right hand, which led to the start of the next trial. In addition, subjects who required more than 15 s for multiple consecutive trials were verbally instructed to reduce processing time. In order to facilitate the learning progress, the 120 objects were presented three times together with the

same cue (i.e., selective horizontal, selective vertical or neutral). The cuing phase consisted of a total number of 360 trials, organized in six blocks.

Finally, the retrieval phase started with the presentation of two circles (size: 2°), together with a central fixation dot. These circles could appear either along the horizontal or the vertical dimension, in accordance with the cued dimension from the second phase. After 500 ms, one of the objects present in the previous phases appeared in the center, between the two circles (distance between the object and the circle in visual angle: 3°) (see Figure 1). Subjects' task was to report the location associated with the object, by clicking with the index finger of the right hand on the corresponding button of the response device. Since the task was generally demanding, we introduced a two-alternative forced-choice task. Accordingly, participants were either presented with the circles on top- and bottom- or on the left- and right locations. The dimension along which these circles appeared always corresponded to the cued axis from the cuing phase. In case of the neutral condition, the probed dimension (vertical or horizontal) was randomly selected, with the restriction that half of the trials cued the horizontal dimension, while the remaining half, the vertical one. The response device was equipped with four buttons, mapped onto the four possible locations on the screen (top, bottom, left, and right). After each response, subjects were instructed to bring their index finger back to the middle location of the device. In addition, after the location report, subjects were also required to rate their confidence in the provided response on a scale from 1 to 4 (1 = really unsure, 2 = relatively unsure, 3 = relatively sure, 4 = very sure).

2.4. Data analyses

All behavioral, EEG, and statistical analyses were conducted in MATLAB® (R2021b). As a first step, each participant's dataset was divided according to the three phases of the task: encoding, cuing, and retrieval. The EEG analyses were conducted only on the cuing phase data.

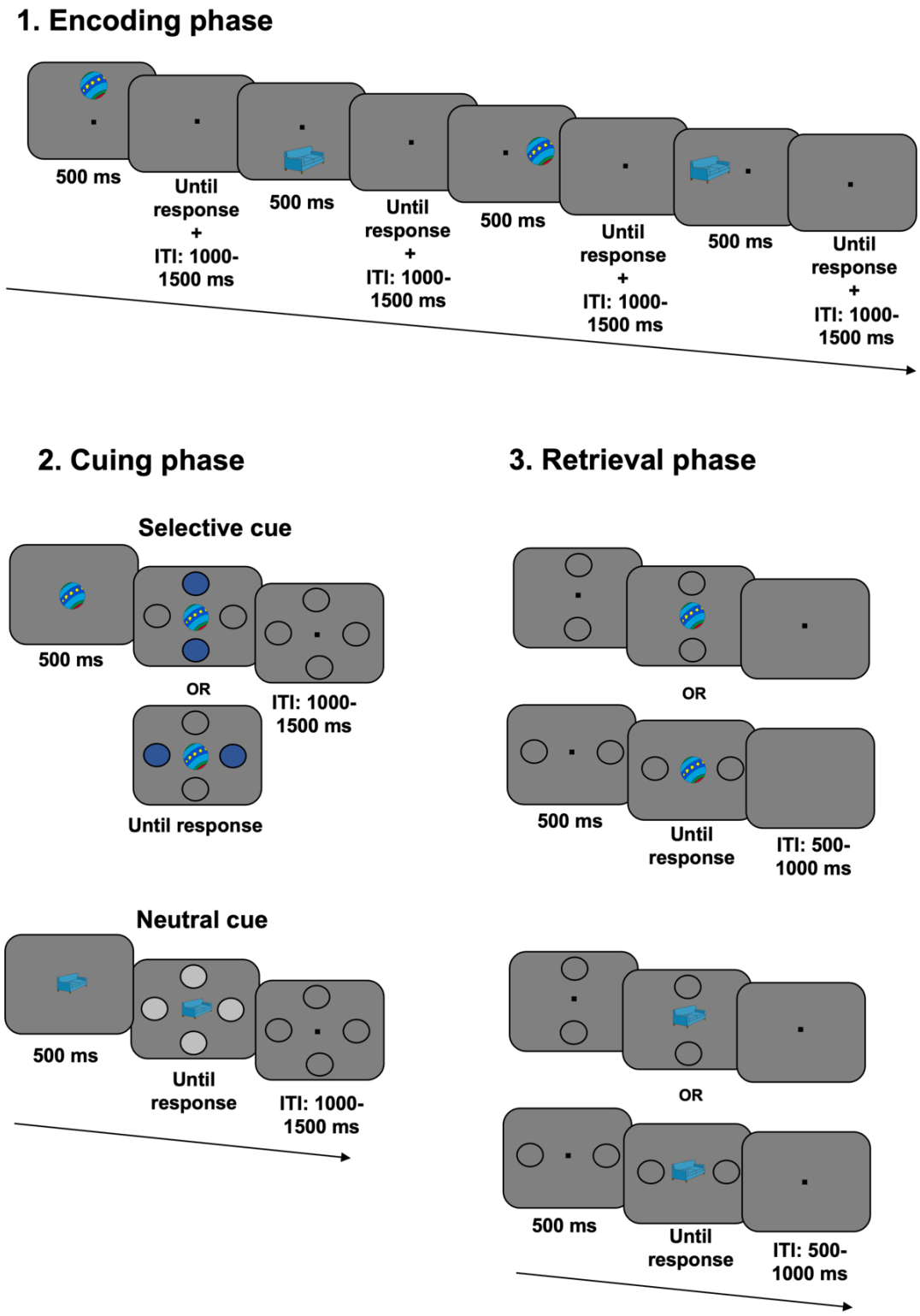

Figure 1. Schematic illustration of the experimental design. In the encoding phase, subjects learnt associations between everyday objects and two locations on the screen. Each trial was self-paced and after subject's response, we introduced an iter-trial interval (ITI) randomly varied between 1000-1500 ms. In the cuing phase, the objects from the previous phase were again presented along with a selective or neutral cue and subject's task

was to either selectively associate only one location with the object (selective cue indicating the horizontal or the vertical axis) or both originally encoded locations. After subject's response, we introduced again an ITI randomly varied between 1000-1500 ms. Finally, in the retrieval phase, subjects were centrally shown the objects and had to report the associated location, according to the indicated axis: horizontal or vertical. The trial ended with an ITI randomly varied between 500-1000 ms.

2.4.1. Behavioral analyses

As part of our behavioral analysis, we first investigated response times recorded during the cuing phase, which reflect the amount of time subjects assigned to think about the selective association between the object and a single location (selective cue condition) or the association between the object and two locations (neutral cue condition). As such, we were interested in how response times differed between the two task conditions. Beyond this condition difference, we also explored how response times changed with object occurrence (i.e., the number of instances during which the same object-cue association was presented; possible occurrences: first, second or third). In order to answer these questions, we conducted a 2 x 3 repeated measures analysis of variance (rm-ANOVA) with the within-subject factors *cue type* (selective vs. neutral) and *occurrence* (first vs. second vs. third).

In the second step, we assessed the accuracy, response time, and confidence ratings during the retrieval phase, when subjects were required to report the location associated with each object. We separated the retrieval trials containing objects previously presented together with a selective cue vs. objects presented together with a neutral cue during the cuing phase. As such, using paired sample t-tests, we examined the differences of each behavioral parameter between these two experimental conditions. When it comes to the confidence rating analysis, we conducted it first for all trials irrespective of correctness and then only for trials with correct responses.

2.4.2. EEG recording

The EEG data were collected with a passive 64 channel Ag/AgCl system (Easycap GmbH, Herrsching, Germany), with its electrode distribution following the extended 10/20

system (Pivik et al., 1993). During recording, the signal was amplified by a NeuroOne Tesla AC-amplifier (Bittium Biosignals Ltd, Kuopio, Finland) and it was low-passed filtered at 250 Hz. The original sampling rate of the data was 1000 Hz and FCz acted as the reference electrode, while AFz served as the ground electrode. Throughout the session, the impedances were kept below 20 kΩ.

2.4.3. Preprocessing

We preprocessed the data using the EEGLAB toolbox (v. 14.1.2b, Delorme & Makeig, 2004) implemented in MATLAB®. Since each analysis required a slight change in the preprocessing parameters, four preprocessing pipelines were developed. We will start by describing these steps for the preprocessing procedure conducted for the lateralized alpha-beta and delta-to-theta analysis. For the remaining pipelines, we will only describe the differently implemented steps.

As a first step in our preprocessing procedure, a 0.1 Hz Hamming windowed sinc FIR high-pass filter (filter order: 33001, transition bandwidth: 0.1 Hz, cutoff frequency at −6 dB: 0.05 Hz) and a 30 Hz low-pass filter (filter order: 441, transition bandwidth: 7.5 Hz, cutoff frequency at −6 dB: 33.75 Hz) were applied (*pop_eegfiltnew* function). Subsequently, channels containing high levels of noise were rejected using the automated channel rejection procedure adopted in EEGLAB (via the *pop_rejchan* function) and data were re-referenced to the average. The anterior channels capturing eye movements (Fp1/2, Fpz, AF3/4, AF7/8, AFz) were excluded from the channel rejection procedure in order to ensure an optimal detection of eye-movement-related components later in the independent component analysis (ICA). The following steps served to prepare the data for the ICA. Data were downsampled to 200 Hz and high-pass filtered using a 1 Hz Hamming windowed sinc FIR filter (*pop_eegfiltnew*, filter order: 661, transition bandwidth: 1 Hz, cutoff frequency at −6 dB: 0.5 Hz). Next, epochs ranging between -1000-3000 ms relative to the object onset were created,

followed by baseline correction (time window of the baseline: -200-0 ms). Subsequently, trials containing extreme fluctuations were rejected via the automated trial rejection procedure of EEGLAB (i.e., *pop_autorej*; threshold: 500 µV, maximum % of rejected trials: 5%). Afterwards, the ICA was performed on the rank-reduced data (remaining number of channels minus 1 - obtained through the principial component analysis built into the *pop_runica* function). In order to identify the independent components (ICs) containing artifacts (e.g., eye movements, muscle activity, channel noise etc.), we used the ICLabel plug-in (v1.3, Pion-Tonachini et al., 2019). ICLabel operates with seven categories (brain, muscle, eye, heart, line noise, channel noise, and other noise) and in case of each IC, it assigns a probability for containing the type of noise described by these categories. For the current analysis, we rejected the ICs which were labelled with a 30% (or more) probability as an eye movement component, as well as those which were labelled with less than 30% probability as a brain component (in accordance with Wascher et al., 2022). Then, the weights obtained from the ICA were written back to the 1000 Hz data, band-pass filtered and re-referenced data. Next, epochs time-locked to the object onset (-1000-3000 ms) were created and data were baseline corrected (-200-0 ms baseline). Afterwards, the ICs marked for rejection were removed and trials still containing large fluctuations were rejected via the same automated procedure mentioned above (threshold: 1000 µV, maximum % of rejected trials: 5%). Finally, using the spherical spline method implemented in EEGLAB (i.e., *pop_interp*), missing channels were interpolated.

Regarding the preprocessing steps of the two ERP analyses (i.e., stimulus-locked and response-locked; see below), we implemented a different IC component rejection criterion. As such, we excluded only those components which were categorized with less than 30% probability as a brain component. This step was adopted, because in our previous investigation (see Sabo & Schneider, 2022) eye movements reflected in the anterior ERPs

were a relevant additional parameter through which the focus of attention could be tracked. In addition, in the stimulus-locked dataset, epochs were created between -1000 and 3000 ms, while in the response-locked analysis, the time window was set to -1500-1500 ms (relative to the response).

Finally, when it comes to preprocessing the data for the decoding analysis (see below), filtering was omitted (except the 1 Hz low-pass filtering meant to prepare the data for the ICA), as it has been previously argued that such filtering can artificially inflate decoding results (van Driel et al., 2021). Moreover, since decoding analyses are sensitive to the input data's trial number, the trial rejection procedure was eliminated from this last pipeline. Finally, since filtering and trial rejection were omitted, we decided to apply channel rejection for the whole range of electrodes.

Table 1

Overview of the outcome of each preprocessing pipeline

Dataset – purpose of the analysis	Rejected number of channels	Number of remaining trials before ICA	Number of rejected IC components	Number of remaining trials after the ICA
Oscillatory power analyses	*M* = 1.53 Range: 0-5	*M* = 303.60 (85.13%) Range: 237-339	*M* = 27.03 Range: 12-40	*M* = 305.96 (85.86 %) Range: 259-353
ERP analysis – stimulus-locked	*M* = 1.60 Range: 0-6	*M* = 306.06 (85.26%) Range: 239-347	*M* = 27.53 Range: 14-43	*M* = 300.76 (83.70%) Range: 247-348
ERP analysis – response-locked	*M* = 1.60 Range: 0-6	*M* = 306.06 (85.26%) Range: 239-347	*M* = 23.96 Range: 10-38	*M* = 293.36 (81.80%) Range: 201-338
Decoding	*M* = 1.43 Range: 0-5	-	*M* = 34.90 Range: 20-47	-

2.4.4. Time-frequency decomposition

After preprocessing, data were downsampled to 250 Hz and two different complex Morlet wavelet convolution analyses were conducted. This procedure relies on convolving the data with a family of complex Morlet wavelets obtained by calculating the timepoint-wise

dot product between complex sine waves of varying frequencies and Gaussians of different widths (as defined by the number of cycles). The first procedure was implemented for the lateralized alpha-beta and delta-to-theta power analyses, therefor our complex Morlet wavelet family covered 18 logarithmically spaced frequencies between 2 and 20 Hz. The number of cycles started at 2 and increased in logarithmic steps until it reached 19 cycles at 20 Hz. Since our decoding analysis was rather exploratory in nature, we aimed to include a broader frequency range, especially because we added frequencies as a feature in our classifier. In this case, the complex Morlet wavelet family covered 26 logarithmically spaced frequencies between 4 and 30 Hz, and the number of cycles started at three and increased in logarithmic steps until 11.25 (at the highest frequency). Finally, for the oscillatory power analyses, baseline normalization was also adopted through decibel conversion, thus the reported power values are in units of decibel (dB). As an additional preparatory step for the decoding procedure, we downsampled the data by selecting every fifth timepoint.

2.4.5. Lateralized alpha-beta oscillations

In order to test our main hypothesis, we investigated modulations of lateralized alpha-beta oscillatory activity. First, we calculated the average contralateral, ipsilateral, and contralateral-minus-ipsilateral activity relative to the lateral target location (selective cue condition) and relative to the lateral non-target location (selective cue condition) for the chosen posterior cluster (PO7/8, P7/8, P5/6). The channel selection procedure was based on a previous investigation conducted in our lab (Sabo & Schneider, 2022). In line with our hypotheses, we compared the contralateral vs. ipsilateral activity from all frequencies and timepoints in the time window 0-2000 ms via a cluster-based permutation procedure. The choice of the upper limit of the time window was again based on our previous investigation (Sabo & Schneider, 2022).

In the adopted cluster-based permutation procedure, each voxel of the original time-frequency data was compared between conditions using paired-sample t-tests. This resulted in a matrix of *p*-values, containing 18x200 values (frequency x time points). If neighboring voxels containing *p*-values exceeding the significance level (i.e., 0.05) were found, the cluster's size was saved. As a next step, the condition labels (i.e., contralateral or ipsilateral) were randomly exchanged within each participant and paired sample t-tests were again conducted for each voxel of the time-frequency data. As before, clusters of significant *p*-values were identified and those containing the largest number of points were saved for the respective iteration. This procedure of re-shuffling the condition labels and identifying the largest cluster was repeated through 1000 iterations. This way, we could obtain a distribution of maximum cluster sizes, necessary to obtain the cutoff based on which significance is determined. Subsequently, if the cluster(s) identified in the original comparison were larger than the 95th percentile of the cluster size distribution, they were considered to be significant.

2.4.6. Delta-to-theta power analysis

In order to investigate potential differences in the delta-to-theta oscillatory power between selective and neutral cue trials, we averaged first the activity belonging to the frontal cluster (F1/2, Fz, FC1/2, F3/4, F5/6). Electrode selection was based on previous studies investigating attentional control within memory (e.g., Ferreira et al., 2019; Zickerick et al., 2021). The statistical comparison of the two conditions was based on the same cluster-based permutation procedure described above.

2.4.7. ERP analysis

In our subsequent ERP analysis, we aimed to further investigate the N2pc and ADAN component, as markers of attentional selection. As a first step in our analyses, we calculated the average contralateral, ipsilateral, and contralateral-minus-ipsilateral activity relative to the

lateral target, lateral non-target, and lateral location in the neutral condition. In case of the N2pc, activity was obtained from PO7/8 electrodes (cf., Luck & Hillyard, 1994), while in case of the ADAN component, the frontal lateral channels, FC3/4, were considered (cf., Schneider et al., 2016). Next, for each of the three conditions, we averaged the contralateral-minus-ipsilateral activity across the time window 300-500 ms after the cue (i.e., 800-1000 ms after the object onset), in order to be able to conduct statistical comparisons. The time window selection was again based on previous WM studies, which identified these attentional effects occurring ~300 ms after the retro-cue presentation (e.g., Günseli et al., 2019; Poch et al., 2018). Once the averages were obtained, they were contrasted using repeated measures one-way ANOVAs, with the within-subject factor condition (with the levels target, non-target, neutral). In cases, where statistical significance was achieved, post-hoc pair-wise comparisons were calculated.

Due to the high variability of response times during the cuing phase (see Supplementary materials), which might have led to an asynchrony in the processes captured by these components, we introduced a second set of ERP analyses, which were conducted on the EEG data time-locked to the response. The adopted steps matched the ones described above, with the only difference that our time window of analysis was set to -100-100 ms around response. The main assumption behind this choice was that the response in the cuing phase describes the timepoint at which subjects were confident that they had encoded sufficiently the object-location association. Therefore, an asymmetry in the EEG signal reflecting this spatial process should be maximal at the time of the response.

2.4.8. Exploratory analysis - decoding procedure

In addition to the analyses mentioned above, we decided to conduct an additional, exploratory multivariate pattern analysis, since this approach is able to capture hidden patterns, which do not become evident via univariate methods. The main aim of the present

decoding procedure was to investigate whether different locations associated with the objects could be decoded based on the scalp distribution of the EEG power. As such, if these location identities can be differentiated based on the EEG patterns, this would involve that the EEG signal contains relevant information characterizing these stimulus features (cf., Grootswagers et al., 2017). Moreover, we sought to test whether differences in decoding accuracy existed between the two conditions (i.e., selective cue- and neutral cue condition). Accordingly, we focused on decoding the target location in the selective cue condition, as well as the target locations from the neutral cue condition. More specifically, in case of the former analysis (selective cue condition), the classifier was trained to distinguish between: (i) left vs. right target locations (i.e., trials, in which the subject was supposed to selectively associate the object with the right location vs. trials, in which the subject was supposed to selectively associate the object with the left location); and (ii) top vs. bottom target locations. The reason for not including other contrasts, such as left vs. top or right vs. bottom was due to the cues differing in their perceptual characteristics. For example, in trials, in which the target location was left, two horizontal colored circles were shown, while in trials with a top target location, two vertical colored circles. Including such contrasts to our analysis would have led to decoding the identity of the cue (i.e., horizontal vs. vertical), instead of decoding the target location. Since in case of the neutral condition, all trials included four gray-colored circles, we were able to train the classifier to differentiate between any combination of four locations: left vs. right, top vs. bottom, top vs. left, top vs. right. bottom vs. left and bottom vs. right. Note however, that we excluded trials, in which the classifier was trained to distinguish between the exact two target locations, which were associated with the object, because this would have led to biased decoding results. Overall, considering these contrasts, the classification routine was ran two times for the selective cue condition and six times for the neutral cue condition. Regarding the decoding analysis pipeline, we adopted the approach

described by Bae and Luck (2018), who used a combined support vector machines (SVM) and error-correcting output codes approach (ECOC; Dietterich & Bakiri, 1994), which is implemented into the *fitcecoc()* MATLAB® function. Testing and model predictions were done via the *predict()* function.

The input to our decoding procedure was constituted by the power values, resulting from the time-frequency decomposition. Since this procedure was an exploratory analysis, with no a-priori assumptions about potential outcomes, we included all the 26 frequency-bands and 64 electrodes as features in our analysis. Classification was executed within each participant and timepoint separately. We focused on the EEG oscillatory activity between -200-2000 ms, containing 126 timepoints. As such, at each timepoint of an iteration, the trials belonging to each of the locations were divided randomly into three groups, from this point on referred to as blocks. An important aspect here was to ensure that an equal number of trials linked to each location was assigned to each block. In cases, in which the trial number could not be divided by three, these additional trials were removed. Within each block, data were averaged within each location label, thus resulting in three averages for each location. In line with the argumentation of Bae and Luck (2018), averaging serves as a good modality to reduce noise, therefor we chose to perform the classification procedure on trial averages rather than single trial data. The model training was done on 2/3 of these averages, while the test was conducted on the remaining 1/3. Since we performed a 3-fold cross-validation, each of these averages served once as a test dataset. Once this procedure was complete, trials were again shuffled and randomly re-assigned to one of the three blocks. Within these blocks, averages were again calculated and labeled as a training or a test dataset. This process was repeated in each of the 10 iterations. Once predicted labels were obtained for all timepoints and iterations within a participant, we calculated the decoding accuracy by comparing the predicted labels to the true ones. Decoding accuracy was subsequently averaged across

iterations and in order to smooth these time series, a five-point moving time window was applied. Finally, decoding accuracies were averaged across participants. Considering that we always contrasted two locations, the chance level was set to 50%.

When it comes to the statistical procedure, we first contrasted the decoding accuracy to chance level, followed by the comparison between conditions. For this, we used the cluster-corrected sign-permutation test described by Wolff et al. (2017). This procedure is based on generating a null distribution by flipping the sign of the values with a 50% probability, throughout 10000 iterations (function: *cluster_test_helper*). Subsequently, using this null distribution, significant clusters are determined in the actual data (function: *cluster_test)*. All significance thresholds were set to $p < .05$. In case of the first statistical comparison, where decoding accuracy was compared to chance level, we ran one-sided cluster-corrected sign-permutation tests, since decoding accuracy was expected to be greater than chance level. The comparison was restricted to the same time window used for the oscillatory analyses, namely 0-2000 ms. In the next step, we contrasted the decoding accuracy of the two conditions against each other, using a two-sided test restricted to the time window 500-2000 ms. The lower limit was set to 500 ms, because we wanted to capture potential effects occurring beyond the early cluster captured by the first statistical procedure. In case of this second time window, we conducted an additional post-hoc comparison, in which decoding accuracy from each condition was separately averaged over the obtained significant cluster and contrasted again chance level via a one-sample t-test.

2.4.9 Inferential statistics and effect sizes

In case of each ANOVA, we tested the sphericity assumption via Mauchly's test for sphericity. When this assumption was violated, we applied the Greenhouse-Geisser correction (denoted with ε) and reported the corresponding corrected *p*-values (p_{corr}). As a measure of effect size, we used Cohen's d_{av} for the paired *t*-tests (following the recommendations of

Lakens, 2013) and partial eta square (η_p^2) for the ANOVAs. If not otherwise specified, statistical significance was set to 0.05. False discovery rate (FDR) corrected *p*-values (p_{adj}) were reported when correction for multiple comparisons was necessary.

3. Results

3.1. Behavioral results

Response times during the cuing phase were assessed in order to investigate whether processing time changed as a function of condition (i.e., selective or neutral) or with each object occurrence (i.e., first, second or third). In addition, we also tested for an interaction effect between these two factors. The results of the 2 x 3 rmANOVA (Figure 2a) yielded a main effect of condition, suggesting that participants were faster in the selective cue ($M_{selective}$ = 2239.93 ms; $SD_{selective}$ = 1068.72 ms), as compared to the neutral cue condition ($M_{neutral}$ = 2584.75 ms; $SD_{neutral}$ = 1309.62 ms): $F(1, 29) = 13.42$, $p < .001$, $\eta_p^2 = 0.31$. In addition, a main effect of occurrence has been observed, with subjects being the slowest during the first object occurrence ($M_{occurrence1}$ = 3020.82 ms; $SD_{occurrence1}$ = 1375.33 ms), followed by the second one ($M_{occurrence2}$ = 2287.65 ms; $SD_{occurrence2}$ = 1151.99 ms) and finally the fastest during the third occurrence of the object ($M_{occurrence3}$ = 1928.56 ms; $SD_{occurrence3}$ = 1075.78 ms: $F(2, 58) = 64.26$, $p_{corr} < .001$, $\eta_p^2 = 0.68$, $\varepsilon = 0.73$. Finally, we also found a significant interaction effect of condition and occurrence: $F(2, 58) = 6.12$, $p = .003$, $\eta_p^2 = 0.17$. The subsequent post-hoc t-tests revealed that the response times significantly differed between selective and neutral trials during the first occurrence ($M_{selective}$ = 2772.52 ms; $SD_{selective}$ = 1200.06 ms; $M_{neutral}$ = 3269.12 ms; $SD_{neutral}$ = 1597.95 ms): $t(29)$: = -4.19, $p_{adj} < .001$, $d_{av} = 0.35$, 95% CI [-738.89 -254.30], and during the second one ($M_{selective}$ = 2120.49 ms; $SD_{selective}$ = 1086.75 ms; $M_{neutral}$ = 2454.80 ms; $SD_{neutral}$ = 1265.24 ms): $t(29)$: = -3.62, p_{adj} = .001, $d_{av} = 0.28$, 95% CI [-523.03 -145.62], but not during the third occurrence ($M_{selective}$ = 1826.78 ms; $SD_{selective}$ = 1019.28 ms; $M_{neutral}$ = 2030.33 ms; $SD_{neutral}$ = 1200.72 ms): $t(29)$: = -

1.93, p_{adj} = .06, d_{av} = 0.18, 95% CI [-418.72 11.63]. This confirms that the response time difference between the two conditions becomes diminished as a function of occurrence.

Furthermore, in order to investigate whether the use of the selective cue resulted in any behavioral benefit during the retrieval phase, we compared response accuracy (measured as the % of correct responses), the response confidence rating and response time between selective and neutral trials. Our results revealed no significant differences in accuracy between the location report linked to the selective trials ($M_{selective}$ = 84.12 %; $SD_{selective}$ = 7.88 %) and the location report in the neutral trials ($M_{neutral}$ = 84.83 %; $SD_{neutral}$ = 8.55 %): $t(29) = -0.61$, $p = 0.54$, $d_{av} = 0.08$, 95% CI [-3.04 1.62] (Figure 2b). When it comes to response times, results showed that subjects were significantly faster in reporting the location of an object occurring in the selective cue condition ($M_{selective}$ = 1425.99 ms; $SD_{selective}$ = 683.82 ms), as compared to the neutral cue condition ($M_{neutral}$ = 1560.89 ms; $SD_{neutral}$ = 685.51 ms): $t(29) = -2.69$, $p = .01$, $d_{av} = 0.19$, 95% CI [-237.30 -32.49] (Figure 2c). Moreover, participants were more confident in their responses in the selective cue condition ($M_{selective}$ = 3.23; $SD_{selective}$ = 0.36) than in the neutral condition ($M_{neutral}$ = 3.15; $SD_{neutral}$ = 0.47): $t(29) = 2.26$, $p = .03$, $d_{av} = 0.19$, 95% CI [0.00 0.15] (see Figure 2d). The same pattern was obtained when only correct trials were considered for the comparison ($M_{selective}$ = 3.37; $SD_{selective}$ = 0.33; $M_{neutral}$ = 3.24; $SD_{neutral}$ = 0.46): $t(29) = 3.27$, $p = .002$, $d_{av} = 0.32$, 95% CI [0.04 0.21] (see Figure 2e). Overall, these results suggest a performance benefit associated with the selective cue in terms of response time and response confidence, but not in terms of accuracy.

3.2. Posterior lateralized alpha-beta activity

Since we were interested to explore the role of attentional selection mechanisms during the cuing phase, we first investigated lateralized oscillatory power in the alpha-beta frequency domain (8-20 Hz). Here, we contrasted the contralateral and ipsilateral activity

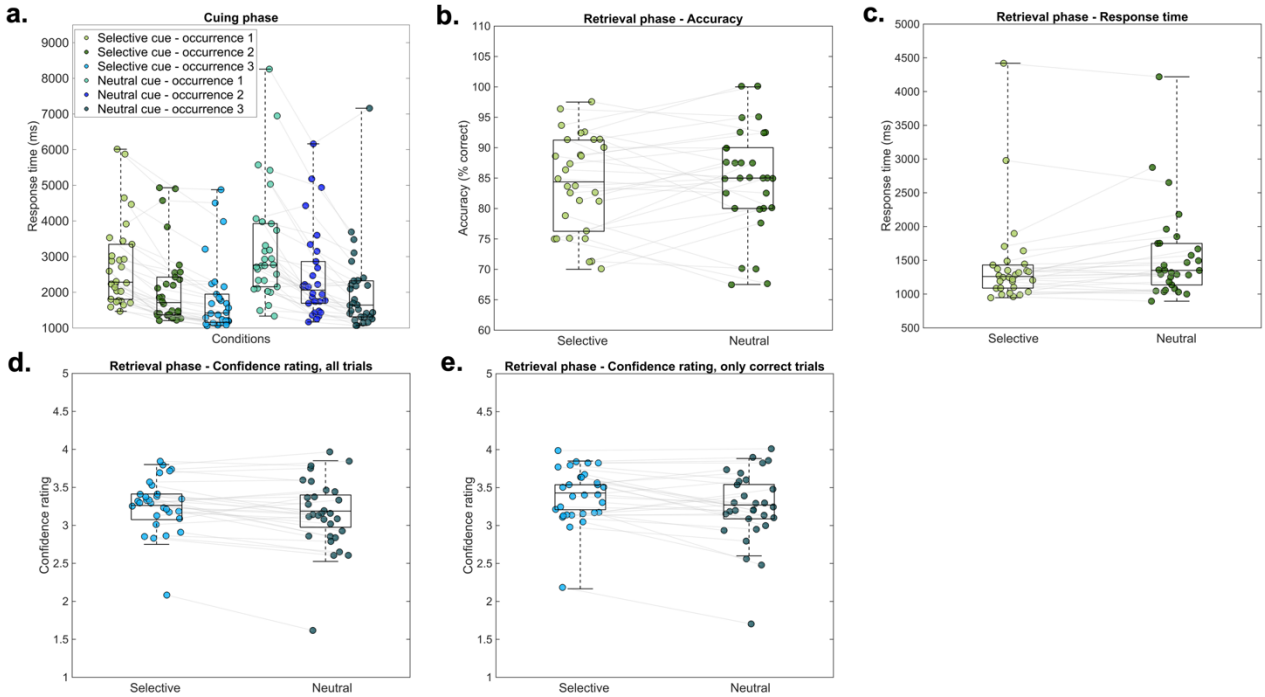

Figure 2. Behavioral results. Scatterplots depicting a. the average reaction time (in ms) of each participant in the cuing phase separated for each condition and occurrence, b. the average accuracy, c. the average response time, d. the average confidence rating (all trials) and e. confidence rating (only correct trials) in the retrieval phase, separated for each condition. The central mark on each boxplot indicates the median, and the bottom and top edges of the box mark the 25th and 75th percentiles. The whiskers are not extended to averages considered outliers. Data points belonging to the same participant are connected via the grey lines.

(electrode cluster: P5/6, P7/8, PO7/8) separately relative to the target and to the non-target location via cluster-based permutation analyses (time window: 500-2000 ms). As shown, in the time-frequency plot depicted in Figure 3, results did not reveal differences between the contralateral and ipsilateral power, either with respect to the target location or with respect to the non-target location.

3.3. Frontal delta-to-theta activity

Beyond the lateralized alpha-beta activity, we also explored changes in the delta-to-theta-band power, as this has previously been argued to track attentional control processes. Figure 4a depicts the results of the cluster-based permutation statistics conducted on the time-frequency data averaged over the frontal electrode cluster (F1/2, Fz, FC1/2, F3/4, F5/6). Compared to the neutral cue condition, results revealed a stronger delta-to-theta power in the

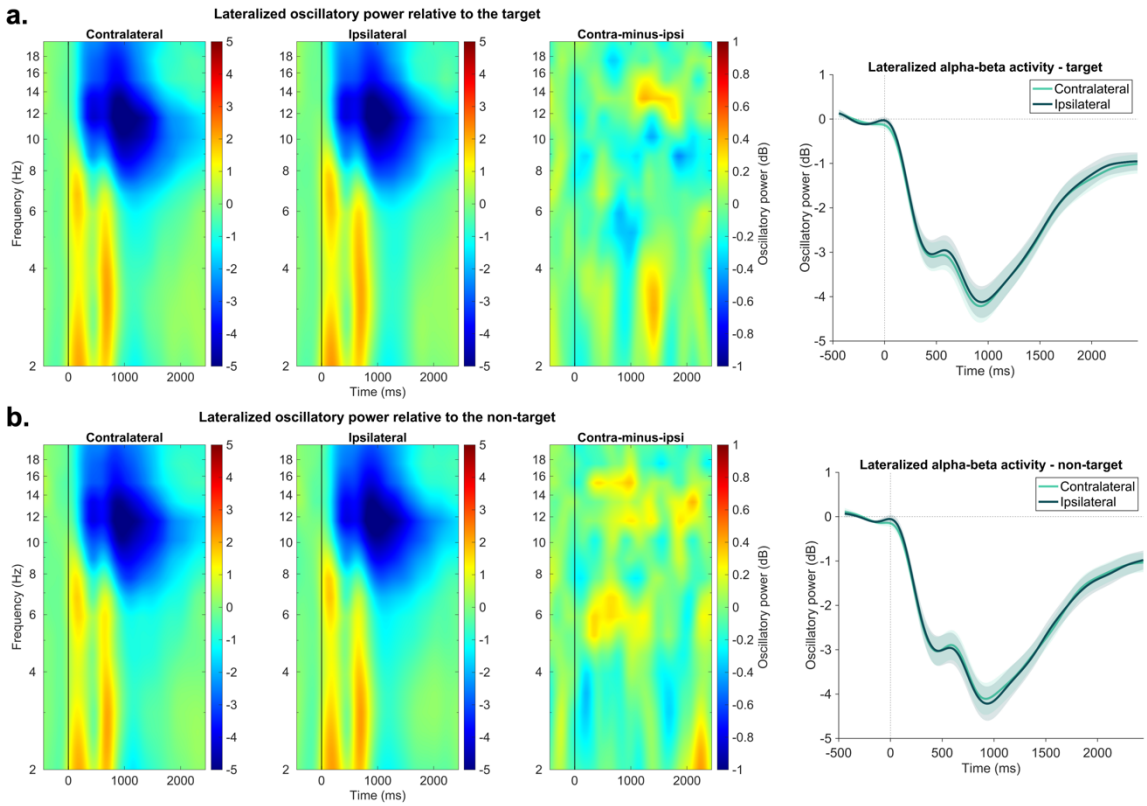

Figure 3. Lateralized alpha-beta power analysis results. The panel on the left side depicts the time-frequency representation of the activity contralateral, ipsilateral and its difference relative to the a. lateral target and b. lateral non-target locations. The activity was obtained from the electrode cluster: P5/6, P7/8, PO7/8. The vertical line (left panel) and dotted vertical line (right panel) at 0 ms indicates the object onset. The right panels show the corresponding line plots obtained by averaging the contralateral and ipsilateral activity across the frequencies 8-20 Hz. The shaded green areas depict the standard error of the mean.

selective cue condition, with the significant cluster at 2-5 Hz, ranging between 72-463 ms relative to the cue presentation (i.e., 572-963 ms relative to objects presentation). As indicated in the topographical representation of the difference activity (Figure 4c), the effect is maximal at frontal and left parietal regions. Since our original hypotheses focused only on the frontal activity, we did not investigate the potential parietal effect further. Finally, it is important to note that these differences in delta-to-theta power between the selective and neutral cue condition are not due to sensory imbalance (i.e., differences rising due to the presentation of two blue circles in the selective condition and four grey circles in the neutral cue condition). If this had been the case, the delta-to-theta power would have been the

strongest in the neutral cue condition, because the cue presented during the neutral condition is more salient. As indicated in figure 4a and 4b, opposite patterns were obtained.

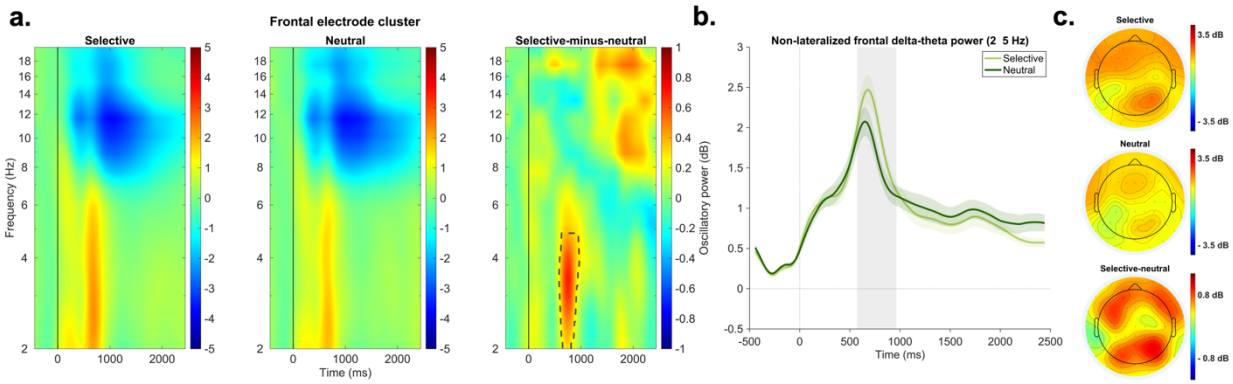

Figure 4. Frontal delta-to-theta-band power results. Panel a illustrates the average time-frequency representation of the frontal activity (F1/2, Fz, FC1/2, F3/4, F5/6) for the selective and neutral conditions, as well as their difference. The black dotted line depicts the significant cluster obtained as a result of the cluster-based permutation procedure (2-5 Hz, 572-963 ms relative to objects presentation). Panel b shows the time course of the delta-to-theta activity, averaged over the significant frequency range, 2-5 Hz. The shaded gray area represents the same time window of significance shown in panel a, while the shaded green areas depict the standard error of the mean. The dotted vertical line (right panel) at 0 ms indicates the object onset. Panel c illustrates the topographical representation of the activity averaged over the 572-963 ms time window for the two conditions and their respective difference.

3.4. Event-related potential analysis

In order to address our main research question, we investigated the N2pc and ADAN as correlates of attentional selection. First, we focused on the ERP effects calculated relative to the stimulus onset. As indicated in Figure 5a, no statistically reliable effects were found in the posterior contralateral-minus-ipsilateral analysis (i.e., N2pc): $F(2, 58) = 2.07$, $p = .13$, $\eta_p^2 = 0.06$. Similarly, when it comes to the ADAN component (electrode cluster FC3/4), our ANOVA results did not yield any significant results: $F(2, 58) = 1.12$, $p = .33$, $\eta_p^2 = 0.03$ (Figure 5b). Overall, this shows that we were not able to find evidence for either N2pc or ADAN effects in our stimulus-locked data.

Since subjects could perform the task of the second phase in a self-paced manner, the time required for different trials within one subject was highly variable (see Supplementary materials). Therefore, it is highly likely that the timing of the processes captured by the ERP components also differed from trial to trial, resulting in the lack of statistically reliable

results. Consequently, as a next step, we performed the same procedure mentioned above for trials time-locked to the response. Please note that in the context of the cuing phase, responses were given by subjects to confirm being done with associating the object with the required location(s).

First, we conducted our analysis for the posterior contralateral-minus-ipsilateral activity. Our ANOVA did not show an effect of condition: $F(2, 58) = 0.36$, $p = .69$, $\eta_p^2 = 0.01$ (Figure 6a). However, when it comes to the analysis conducted for the response-locked anterior activity, our ANOVA revealed a main effect of condition: $F(2, 58) = 3.55$, $p = .03$, $\eta_p^2 = 0.10$. The post-hoc comparisons yielded a stronger negative-going deflection relative to the target as compared to the non-target location: $t(29)$: = -2.60, $p_{adj} = .04$, $d_{av} = 0.74$, 95% CI [-1.46 -0.17]. The target vs. neutral contrasts showed a statistical trend: $t(29)$: = -1.95, $p_{adj} = .09$, $d_{av} = 0.39$, 95% CI [-1.22 0.02], while the non-target vs. neutral comparison did not produce significant results: $t(29)$: = -0.67, $p_{adj} = .50$, $d_{av} = 0.18$, 95% CI [-0.90 0.45] (Figure 6b). Overall, these results show that the anterior contralateral-minus-ipsilateral activity differs between conditions. Nevertheless, in order to make definite claims about attentional selection mechanisms present in case of the target location, a further statistical test has to confirm that the contralateral-ipsilateral difference wave is significantly lower than zero. The follow-up one-sample t-test we conducted showed that this is the case: $t(29)$: = -4.00, $p < .001$, 95% CI [-1.53 -0.49] (see also Figure 6b). To summarize, these results suggests that the target location was subjected to attentional selection before the subject provided a response. Moreover, the difference we found between the target vs. non-target activity confirms that this selection process happens only relative to the target, but not relative to the lateral non-target location.

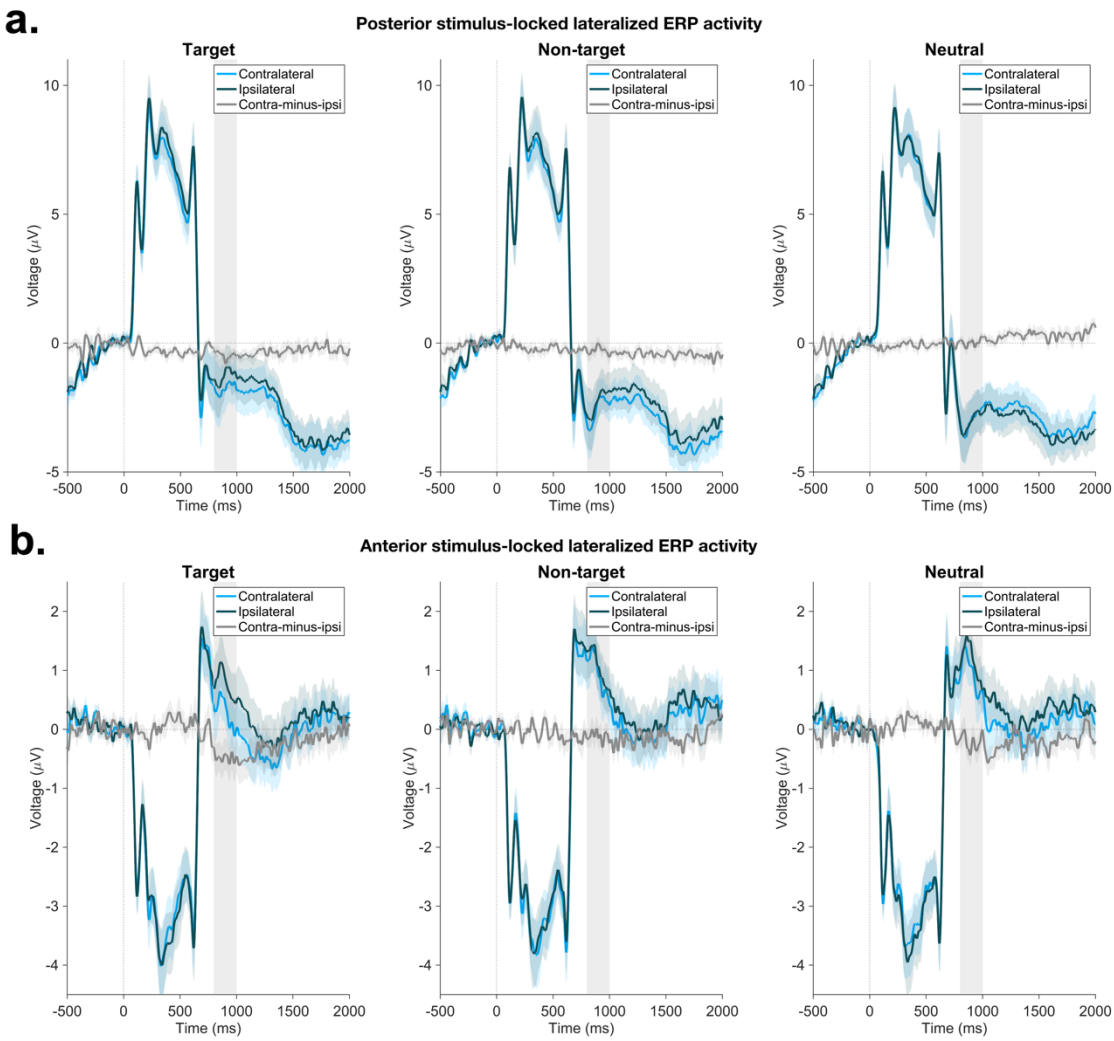

Figure 5. ERP results of the stimulus-locked analyses. Panel a represents the posterior contralateral, ipsilateral, and contralateral-minus-ipsilateral activity relative to the lateral target (left), lateral non-target location (middle), and lateral locations in the neutral condition (right). The activity was obtained from the electrodes PO7/8. Panel b reflects the same asymmetries, obtained from electrodes FC3/4. The grey area represents the time window (750-1000 ms) used for the statistical analyses. The shaded blue areas depict the standard error of the mean.

3.5. Decoding analysis

Figure 7 illustrates the comparison of average decoding accuracy between the selective and neutral conditions. The classifier was trained to differentiate between target locations based on the scalp distribution of the EEG oscillatory power (see further details in Methods). As a first step, we contrasted the decoding accuracy associated to each condition to chance level (0.5; time window of analysis: 0-2000 ms). Our statistical procedure revealed that decoding accuracy differs significantly from chance level for both conditions, with the significant clusters ranging between 20-300 ms (selective cue condition) and 300-540 ms

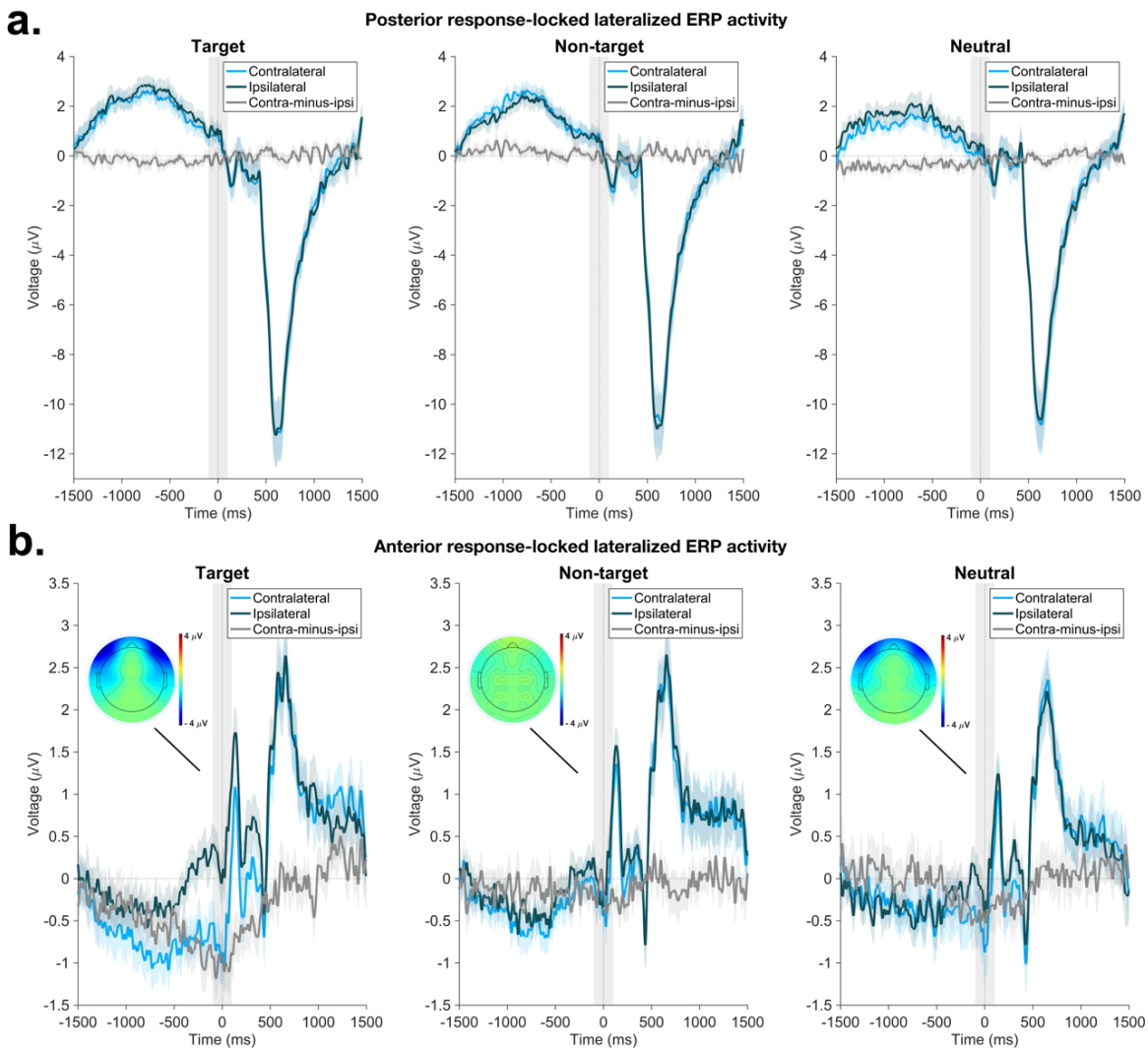

Figure 6. ERP results of the response-locked analyses. Panel a represents the posterior contralateral, ipsilateral, and contralateral-minus-ipsilateral activity relative to the condition with a lateral target (left) and lateral non-target location (middle), and lateral locations in the neutral condition (right). The activity was obtained from the electrodes PO7/8. Panel b reflects the same asymmetries, obtained from electrodes FC3/4. The grey area represents the time window (-100-100 ms) used for the statistical analyses. The topographical representations reflect averages from this time window of analysis. The shaded blue areas depict the standard error of the mean.

(neutral cue condition). This might suggest an early automatic reactivation of the task-relevant location during object presentation. In a next step, we compared the decoding accuracy of the selective vs. neutral trials (time window of analysis: 500-2000 ms) and found that the decoding accuracy differs between conditions, with a significant cluster ranging between 1140-1380 ms. The post-hoc tests revealed that the average activity obtained from this significant cluster significantly differs from chance level in case of the selective target condition (M_{target} = 0.54; SD_{target} = 0.07): $t(29)$: = 3.00, p = .005, 95% CI [0.51 0.56], but not

in case of the neutral condition ($M_{neutral}$ = 0.47; $SD_{neutral}$ = 0.08): $t(29)$: = -1.41, p = .16, 95% CI [0.44 0.50]. This indicates that in comparison with the neutral cue condition, the target location undergoes additional selective processing.

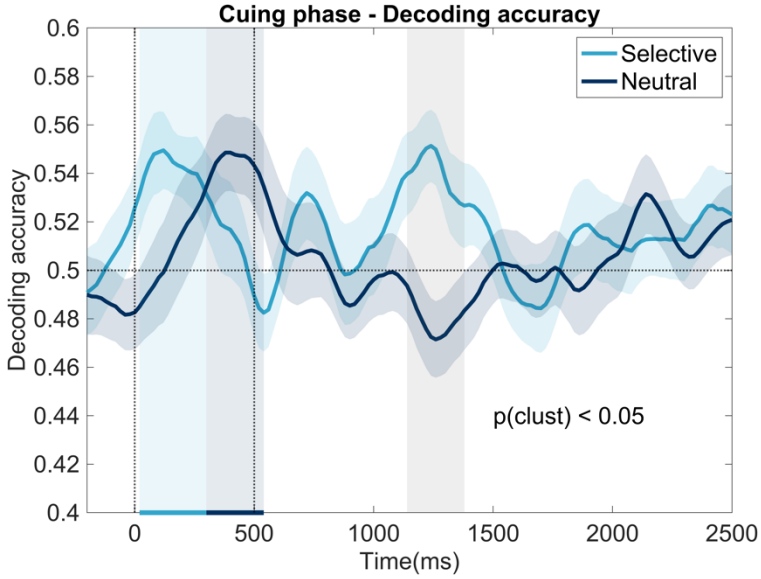

Figure 7. Decoding analysis results. The figure shows the average decoding accuracy over time separately for neutral and selective (target) conditions. The first blue shaded area represents the time window of significance when contrasting the decoding accuracy in the selective condition to chance level (significant cluster: 20-300 ms). The second blue shaded area shows the same outcome, but in case of the neutral condition (significant cluster: 300-540 ms). Finally, the grey shaded area reflects the significant cluster obtained when contrasting the decoding accuracy for the two conditions against each other (1140-1380 ms). The shaded blue area around the decoding accuracy time series depicts the standard error of the mean.

4. Discussion

In the current study, we sought to shed light on whether and how attentional selection is involved in goal-directed memory reactivation. To address this issue, we designed an eLTM experiment, during which we recorded high-temporal resolution brain activity on the level of scalp topography. In our task, subjects encoded associations between an object and two locations on the screen. In order to be able to investigate how different processes modulate goal-directed memory reactivation, we introduced a relevance manipulation in the second phase, involving a change in the behavioral goal. Accordingly, participants were required to retrieve and associate with the object only one of the two initially encoded locations (selective cue condition). Brain activity recorded during this condition was

subsequently contrasted with the activity of the neutral cue condition, in which both originally encoded locations were relevant and thus no change in behavioral goal was required. According to our EEG hypotheses, if attentional selection does indeed play a role during goal-directed memory retrieval, this should be evident in the EEG correlates previously linked to changes in the focus of attention: lateralized alpha-beta oscillations, as well as ERP components, such as the N2pc and ADAN.

Behavioral results from the cuing phase indicated that subjects required less time in trials, in which the object was associated with a single location (selective condition), as compared to trials, in which both locations were still relevant (neutral condition). Nevertheless, this difference diminished over object repetitions, such that by the third object occurrence, subjects needed approximately the same amount of time for the selective and neutral cue trials, suggesting that the learning process was successful. This result is not surprising, since previous studies showed that compared to re-studying a material, retrieval of this information leads to better consolidation, increased subsequent memory performance (Pastötter et al., 2011), and a stronger resistance against interference (Szpunar et al., 2009). In the context of the current task, the adaptation to the new set of goals required participants to retrieve and strengthen only the relevant association, resulting thus in a successful learning outcome.

When it comes to response time during the retrieval phase, we found that subjects provided faster responses for objects from the selective cue condition (i.e., those occurring together with a selective cue during the second phase) as compared to the objects from the neutral cue condition (i.e., those occurring together with a neutral cue during the second phase). We argue that this pattern of results can be explained by the fact that in the selective cue condition, subjects completed already the relevant location selection during the previous phase. However, when it comes to the neutral cue condition, this selection process occurs

only in the retrieval phase, as subjects do not know beforehand which location will be relevant. Moreover, this response time effect obtained at the behavioral level is comparable to the retro-cue effect observed in WM paradigms. Accordingly, when WM items are validly cued during the maintenance period, behavioral performance increases more in comparison with memory items linked to no- or uninformative cues (Griffin & Nobre, 2003; Souza & Oberauer, 2016). Moreover, it was shown that the presence of informative retro-cues results in an automatic shift of attention towards the cued item, which is reflected in modulations of lateralized alpha activity (de Vries et al., 2017; Günseli et al., 2019; Schneider et al., 2019). Overall, the behavioral results show that participants were successful in learning and strengthening the relevant associations and this process might have been facilitated by a potential attentional selection mechanism.

At the EEG level, three important results were found. First, our ERP analysis revealed an anterior asymmetry time-locked to the subject's response, strongest relative to the lateral target location. We interpret this finding as evidence for attentional selection mechanisms acting upon reactivated memory content in the second part of the trial. Although our experiment was specifically designed in a way that allowed subjects to first reactivate the location information and only 500 ms later (with the occurrence of the cue) select the task-relevant information, the fact that the asymmetry peaked around the response indicates that this process was completed in a rather late time window. Since our results yielded a difference between the asymmetry relative to the target condition and the asymmetry relative to the non-target condition, this confirms that the selection process was present only for the target location and did not occur relative to any other lateralized information within the selective cue condition. Our interpretation of the ADAN effect is again in line with previous studies showing that this component tracks changes in the focus of attention within WM (e.g., (Myers et al., 2015; Schneider et al., 2016).

Secondly, our explorative decoding analysis revealed that soon after object presentation, the relevant location associated with each object becomes decodable, possibly reflecting an early reactivation process, which occurs for both the locations in the neutral condition and those in the selective condition. However, in the latter case, we observed a second increase in decoding accuracy, occurring only relative to the selectively cued location. We argue that this pattern can be interpreted as the target location undergoing an attentional selection process, through which the association is strengthened. Since the neutral condition does not require such updating, items in this case are initially reactivated, but re-enter subsequently a de-activated state, because no attentional manipulation is required. This interpretation is also in line with studies showing that information in the focus of attention is decodable, while items not relevant for the ongoing task (i.e., outside the focus of attention) show chance or below chance decoding and are thus retained in an activity-silent state (LaRocque et al., 2013; Rose et al., 2016). As such, it seems plausible that after initial reactivation, the locations in the neutral condition enter an activity-silent state, which might correspond to the process of being placed outside the focus of attention within the activated portion of long-term memory (cf., Kamiński & Rutishauser, 2020).

Finally, we observed a strong difference in the delta-to-theta frequency power between the selective vs. neutral cue condition, with a stronger activity in the selective, as compared to the neutral cue condition. In light of the previous ADAN and decoding results, it is reasonable to expect that this activity reflects control mechanisms, aiming to orchestrate the allocation of attentional resources. More specifically, we argue that in the selective cue condition, subjects require more control, in order to facilitate the successful selection of the task-relevant location. This interpretation would be in agreement with previous findings arguing for the existence of a general control mechanism active during eLTM retrieval and previously shown to be reflected by mid-frontal theta power changes (e.g., Khader & Rösler,

2011) and prefrontal cortex activations (Tarder-Stoll et al., 2020). Overall, the current findings indicate that attentional selection mechanisms underlie the relevance changes occurring in the selective cue condition. Moreover, these attentional processes seem to appear in the second part of the trial (i.e., around the time of response) and show a close resemblance to the processes previously observed in WM paradigms.

In our view, this intriguing similarity emerges as a consequence of attentional reorienting unfolding at the level of WM after initial retrieval from eLTM. In other words, our results suggest that eLTM retrieval requires WM, where retrieved information is temporarily stored and manipulated according to current task demands. As such, locations associated with each object are first reactivated independently of their relevance. Later, with the appearance of the cue, relevant associations are selectively strengthened at the level of WM via attentional processes. The dissociation between this initial reactivation and the subsequent manipulation processes is supported by the two-stage retrieval model proposed by Moscovitch (2008), which suggests that the first step of retrieval is an unconscious, automatic content reactivation, followed by a more effortful, deliberate processing, which is in line with the behavioral goals.

Our current interpretation is also supported by the Embedded Process Model, which assumes that once information is retrieved from eLTM, it enters an activated state (activated part of LTM). From here, a sub-set of the information can be moved into the focus of attention, where further active processing might take place (Cowan et al., 2021). Further evidence for our interpretation comes from previous empirical evidence in favor of the idea that retrieved eLTM content is manipulated at the level of WM (Fukuda & Woodman, 2017). Accordingly, after initial LTM retrieval, the authors showed that subjects either removed some of the initially encoded information, or combined separately encoded items into a single memory representation – both processes being argued to happen at the level of WM. Finally,

recent results point out a striking similarity between the representational format of retrieved LTM content and WM maintenance in parietal regions (Vo et al., 2021), suggesting the possibility that LTM retrieval is realized via the temporary storage of information in WM.

4.1 Conclusions

To summarize, in the current study we tested the question of whether and how attentional selection mechanisms are involved during goal-directed memory reactivation. Although some previous review papers (e.g., Ataseven et al., preprint.; Tarder-Stoll et al., 2020) refer to the role of attentional mechanisms in eLTM retrieval as an established phenomenon, in our view, empirical evidence supporting this claim has been rather scarce in the past. Therefore, we argue that the current investigation contributes to this debate with corresponding empirical evidence, as well as important new insights. First of all, we did not only find evidence for attentional selection mechanisms mediating goal-directed memory reactivation, but also explored the time course of the processes unfolding during eLTM retrieval. More specifically, we could show that these attentional processes are active in a rather late time window (i.e., around the response time of each subject), following initial memory reactivation. Secondly, the EEG correlates, whose modulations we observed in our task, were also previously associated with attentional reorienting within WM, which we interpret as evidence for the observed attentional processes unfolding at the level of WM. Finally, we argue that the present findings have important theoretical implications with respect to the mutual information exchange between the short-term and long-term memory systems. As such, future theoretical models explaining eLTM retrieval sub-processes should also emphasize the role played by the WM system, in supporting post-retrieval processes, such as attentional selection.

Acknowledgments

The authors would like to thank Tobias Blanke for the offered technical support; Karin Lukaszewski for the help with participant recruiting; Pia Deltenre and Barbara Foschi for the lab organisation, and all the students, for contributing to the process of data collection: Joel Althoff, Lara Bleckmann, Nina Cialone, Quang Dang, Patrick Frenken, Kagan Kemerioglu, Vivek Mishra, Vivien Szczepanski, Stefan Weber.

Funding

This work was supported by the German Research Foundation (*Deutsche Forschungsgemeinschaft*; grant number SCHN 1450/2-1).

Author contribution

M.S.: data collection and data analysis. M.S. and D.S.: conceptualisation and writing the original draft. D.S.: project supervision and acquiring the necessary funding. E.W.: supervision and writing (review & editing).

Data availability statement

The raw data and all the scripts used for the reported analyses are publicly available (after publication) on Open Science Framework (OSF): https://osf.io/p93gm/?view_only=44c1ea1c47d0436795e70dd83c89d752

Declaration of Competing Interest

None.

References

Ataseven, N., Ünver, N., & Günseli, E. (preprint). How does divided attention hinder different stages of episodic memory retrieval? https://doi.org/10.31234/osf.io/839by

Bae, G.-Y., & Luck, S. J. (2018). Dissociable Decoding of Spatial Attention and Working Memory from EEG Oscillations and Sustained Potentials. *The Journal of Neuroscience*,

38(2), 409 LP – 422. https://doi.org/10.1523/JNEUROSCI.2860-17.2017

Cavanagh, & Frank, M. J. (2014). Frontal Theta as a Mechanism for Affective and Effective Control. *Trends in Cognitive Sciences*, *18*(8), 414–421. https://doi.org/10.1016/j.tics.2014.04.012.Frontal

Ciaramelli, E., Burianová, H., Vallesi, A., Cabeza, R., & Moscovitch, M. (2020). Functional Interplay Between Posterior Parietal Cortex and Hippocampus During Detection of Memory Targets and Non-targets. *Frontiers in Neuroscience*, *14*(November). https://doi.org/10.3389/fnins.2020.563768

Cooper, P. S., Wong, A. S. W., McKewen, M., Michie, P. T., & Karayanidis, F. (2017). Frontoparietal theta oscillations during proactive control are associated with goal-updating and reduced behavioral variability. *Biological Psychology*, *129*, 253–264. https://doi.org/https://doi.org/10.1016/j.biopsycho.2017.09.008

Cowan, N., Morey, C. C., & Naveh-Benjamin, M. (2021). An Embedded-Processes Approach to Working Memory. In H. R. Logie, V. Camos, & N. Cowan (Eds.), *Working Memory: The state of the science* (First Edit, pp. 44–76). Oxford University Press. https://doi.org/10.1093/oso/9780198842286.001.0001

de Vries, I. E. J., Van Driel, J., Karacaoglu, M., & Olivers, C. N. L. (2018). Priority Switches in Visual Working Memory are Supported by Frontal Delta and Posterior Alpha Interactions. *Cerebral Cortex*, *28*(11), 4090–4104. https://doi.org/10.1093/cercor/bhy223

de Vries, I. E. J., van Driel, J., & Olivers, C. N. L. (2017). Posterior α EEG dynamics dissociate current from future goals in working memory-guided visual search. *Journal of Neuroscience*, *37*(6), 1591–1603. https://doi.org/10.1523/JNEUROSCI.2945-16.2016

Delorme, A., & Makeig, S. (2004). EEGLAB: an open source toolbox for analysis of single-trial EEG dynamics including independent component analysis. *Journal of Neuroscience*

Methods, *134*(1), 9–21. https://doi.org/https://doi.org/10.1016/j.jneumeth.2003.10.009

Dietterich, T. G., & Bakiri, G. (1994). Solving multiclass learning problems via error-correcting output codes. *Journal of Artificial Intelligence Research*, *2*, 263–286.

Eimer, M., Velzen, J. van, & Driver, J. (2002). Cross-Modal Interactions between Audition, Touch, and Vision in Endogenous Spatial Attention: ERP Evidence on Preparatory States and Sensory Modulations. *Journal of Cognitive Neuroscience*, *14*(2), 254–271. https://doi.org/10.1162/089892902317236885

Ferreira, C. S., Maraver, M. J., Hanslmayr, S., & Bajo, T. (2019). Theta oscillations show impaired interference detection in older adults during selective memory retrieval. *Scientific Reports*, *9*(1), 9977. https://doi.org/10.1038/s41598-019-46214-8

Fukuda, K., & Woodman, G. F. (2017). Visual working memory buffers information retrieved from visual long-term memory. *Proceedings of the National Academy of Sciences of the United States of America*, *114*(20), 5306–5311. https://doi.org/10.1073/pnas.1617874114

Griffin, I. C., & Nobre, A. C. (2003). Orienting Attention to Locations in Internal Representations. *Journal of Cognitive Neuroscience*, *15*(8), 1176–1194. https://doi.org/10.1162/089892903322598139

Grootswagers, T., Wardle, S. G., & Carlson, T. A. (2017). Decoding Dynamic Brain Patterns from Evoked Responses: A Tutorial on Multivariate Pattern Analysis Applied to Time Series Neuroimaging Data. *Journal of Cognitive Neuroscience*, *29*(4), 677–697. https://doi.org/10.1162/jocn_a_01068

Günseli, E., Fahrenfort, J. J., van Moorselaar, D., Daoultzis, K. C., Meeter, M., & Olivers, C. N. L. (2019). EEG dynamics reveal a dissociation between storage and selective attention within working memory. *Scientific Reports*, *9*(1), 1–13. https://doi.org/10.1038/s41598-019-49577-0

Jost, K., Khader, P. H., Düsel, P., Richter, F. R., Rohde, K. B., Bien, S., & Rösler, F. (2012). Controlling conflict from interfering long-term memory representations. *Journal of Cognitive Neuroscience*, *24*(5), 1173–1190. https://doi.org/10.1162/jocn_a_00199

Kamiński, J., & Rutishauser, U. (2020). Between persistently active and activity-silent frameworks: novel vistas on the cellular basis of working memory. *Annals of the New York Academy of Sciences*, *1464*(1), 64–75. https://doi.org/https://doi.org/10.1111/nyas.14213

Khader, P. H., & Rösler, F. (2011). EEG power changes reflect distinct mechanisms during long-term memory retrieval. *Psychophysiology*, *48*(3), 362–369. https://doi.org/10.1111/j.1469-8986.2010.01063.x

Kizilirmak, J. M., Rösler, F., Bien, S., & Khader, P. H. (2015). Inferior parietal and right frontal contributions to trial-by-trial adaptations of attention to memory. *Brain Research*, *1614*, 14–27. https://doi.org/10.1016/j.brainres.2015.04.012

Kuhl, B. A., Johnson, M. K., & Chun, M. M. (2013). Dissociable neural mechanisms for goal-directed versus incidental memory reactivation. *Journal of Neuroscience*, *33*(41), 16099–16109. https://doi.org/10.1523/JNEUROSCI.0207-13.2013

Lakens, D. (2013). Calculating and reporting effect sizes to facilitate cumulative science: A practical primer for t-tests and ANOVAs. *Frontiers in Psychology*, *4*(NOV), 1–12. https://doi.org/10.3389/fpsyg.2013.00863

LaRocque, J. J., Lewis-Peacock, J. A., Drysdale, A. T., Oberauer, K., & Postle, B. R. (2013). Decoding attended information in short-term memory: An EEG study. *Journal of Cognitive Neuroscience*, *25*(1), 127–142. https://doi.org/10.1162/jocn_a_00305

Long, N. M., & Kuhl, B. A. (2018). Bottom-up and top-down factors differentially influence stimulus representations across large-scale attentional networks. *Journal of Neuroscience*, *38*(10), 2495–2504. https://doi.org/10.1523/JNEUROSCI.2724-17.2018

Luck, S. J., & Hillyard, S. A. (1994). Electrophysiological correlates of feature analysis during visual search. *Psychophysiology*, *31*(3), 291–308. https://doi.org/10.1111/j.1469-8986.1994.tb02218.x

Moscovitch, M. (2008). The hippocampus as a "stupid," domain-specific module: Implications for theories of recent and remote memory, and of imagination. *Canadian Journal of Experimental Psychology*, *62*(1), 62–79. https://doi.org/10.1037/1196-1961.62.1.62

Myers, N. E., Walther, L., Wallis, G., Stokes, M. G., & Nobre, A. C. (2015). Temporal Dynamics of Attention during Encoding versus Maintenance of Working Memory: Complementary Views from Event-related Potentials and Alpha-band Oscillations. *Journal of Cognitive Neuroscience*, *27*(3), 492–508. https://doi.org/10.1162/jocn_a_00727

Oldfield, R. C. (1971). The Assessment And Analysis Of Handedness: The Edinburgh Inventory. *Neuropsychologia*, *9*, 97–113. https://doi.org/10.1007/978-0-387-79948-3_6053

Pastötter, B., Schicker, S., Niedernhuber, J., & Bäuml, K.-H. T. (2011). Retrieval during learning facilitates subsequent memory encoding. *Journal of Experimental Psychology. Learning, Memory, and Cognition*, *37*(2), 287–297. https://doi.org/10.1037/a0021801

Pion-Tonachini, L., Kreutz-Delgado, K., & Makeig, S. (2019). ICLabel: An automated electroencephalographic independent component classifier, dataset, and website. *NeuroImage*, *198*, 181–197. https://doi.org/https://doi.org/10.1016/j.neuroimage.2019.05.026

Pivik, R. T., Broughton, R. J., Coppola, R., Davidson, R. J., Fox, N., & Nuwer, M. R. (1993). Guidelines for the recording and quantitative analysis of electroencephalographic activity in research contexts. *Psychophysiology*, *30*(6), 547–558.

https://doi.org/10.1111/j.1469-8986.1993.tb02081.x

Poch, C., Valdivia, M., Capilla, A., Hinojosa, J. A., & Campo, P. (2018). Suppression of no-longer relevant information in Working Memory: An alpha-power related mechanism? *Biological Psychology*, *135*, 112–116. https://doi.org/https://doi.org/10.1016/j.biopsycho.2018.03.009

Rose, N. S., Larocque, J. J., Riggall, A. C., Gosseries, O., Starrett, M. J., Meyering, E. E., & Postle, B. R. (2016). *magnetic stimulation*. *354*(6316), 1136–1140.

Rösner, M., Arnau, S., Skiba, I., Wascher, E., & Schneider, D. (2020). The spatial orienting of the focus of attention in working memory makes use of inhibition: Evidence by hemispheric asymmetries in posterior alpha oscillations. *Neuropsychologia*, *142*(March). https://doi.org/10.1016/j.neuropsychologia.2020.107442

Rossion, B., & Pourtois, G. (2004). Revisiting Snodgrass and Vanderwart's Object Pictorial Set: The Role of Surface Detail in Basic-Level Object Recognition. *Perception*, *33*(2), 217–236. https://doi.org/10.1068/p5117

Sabo, M., & Schneider, D. (2022). Pattern reinstatement and attentional control overlap during episodic long-term memory retrieval. *Scientific Reports*, *12*(1), 10739. https://doi.org/10.1038/s41598-022-14090-4

Salahub, C., Lockhart, H. A., Dube, B., Al-Aidroos, N., & Emrich, S. M. (2019). Electrophysiological correlates of the flexible allocation of visual working memory resources. *Scientific Reports*, *9*(1), 1–11. https://doi.org/10.1038/s41598-019-55948-4

Schneider, D., Göddertz, A., Haase, H., Hickey, C., & Wascher, E. (2019). Hemispheric asymmetries in EEG alpha oscillations indicate active inhibition during attentional orienting within working memory. *Behavioural Brain Research*, *359*, 38–46. https://doi.org/10.1016/j.bbr.2018.10.020

Schneider, D., Herbst, S. K., Klatt, L. I., & Wöstmann, M. (2022). Target enhancement or

distractor suppression? Functionally distinct alpha oscillations form the basis of attention. *European Journal of Neuroscience*, *55*(11–12), 3256–3265. https://doi.org/10.1111/ejn.15309

Schneider, D., Mertes, C., & Wascher, E. (2016). The time course of visuo-spatial working memory updating revealed by a retro-cuing paradigm. *Scientific Reports*, *6*(October 2015), 1–12. https://doi.org/10.1038/srep21442

Sestieri, C., Shulman, G. L., & Corbetta, M. (2017). The contribution of the human posterior parietal cortex to episodic memory. *Nature Reviews Neuroscience*, *18*(3), 183–192. https://doi.org/10.1038/nrn.2017.6

Souza, A. S., & Oberauer, K. (2016). In search of the focus of attention in working memory: 13 years of the retro-cue effect. *Attention, Perception, and Psychophysics*, *78*(7), 1839–1860. https://doi.org/10.3758/s13414-016-1108-5

Szpunar, K. K., McDermott, K. B., & Roedigger III, H. L. (2009). "Testing during study insulates against the buildup of proactive interference": Correction. *Journal of Experimental Psychology: Learning, Memory, and Cognition*, *35*, 156. https://doi.org/10.1037/a0014896

Tarder-Stoll, H., Jayakumar, M., Dimsdale-Zucker, H. R., Günseli, E., & Aly, M. (2020). Dynamic internal states shape memory retrieval. *Neuropsychologia*, *138*(July 2019), 107328. https://doi.org/10.1016/j.neuropsychologia.2019.107328

van Driel, J., Olivers, C. N. L., & Fahrenfort, J. J. (2021). High-pass filtering artifacts in multivariate classification of neural time series data. *Journal of Neuroscience Methods*, *352*, 109080. https://doi.org/https://doi.org/10.1016/j.jneumeth.2021.109080

Vo, V. A., Sutterer, D. W., Foster, J. J., Sprague, T. C., Awh, E., & Serences, J. T. (2021). Shared Representational Formats for Information Maintained in Working Memory and Information Retrieved from Long-Term Memory. *Cerebral Cortex*, 1–16.

https://doi.org/10.1093/cercor/bhab267

Waldhauser, G. T., Johansson, M., & Hanslmayr, S. (2012). Alpha/beta oscillations indicate inhibition of interfering visual memories. *Journal of Neuroscience*, *32*(6), 1953–1961. https://doi.org/10.1523/JNEUROSCI.4201-11.2012

Wascher, E., Sharifian, F., Gutberlet, M., Schneider, D., Getzmann, S., & Arnau, S. (2022). Mental chronometry in big noisy data. *PLOS ONE*, *17*(6), e0268916. https://doi.org/10.1371/journal.pone.0268916

Wolff, M. J., Jochim, J., Akyürek, E. G., & Stokes, M. G. (2017). Dynamic hidden states underlying working-memory-guided behavior. *Nature Neuroscience*, *20*(6), 864–871. https://doi.org/10.1038/nn.4546

Zickerick, B., Rösner, M., Sabo, M., & Schneider, D. (2021). How to refocus attention on working memory representations following interruptions—Evidence from frontal theta and posterior alpha oscillations. *European Journal of Neuroscience*, *54*(11), 7820–7838. https://doi.org/https://doi.org/10.1111/ejn.15506